



HAL
open science

Integrity of helix 2-helix 3 domain of the PrP protein is not mandatory for prion replication

Muhammad Khalid Salamat, Mohammed M. Moudjou, Jerome Chapuis, Laetitia Herzog, Emilie Jaumain, Vincent Béringue, Human Rezaei, Annalisa Pastore, Hubert H. Laude, Michel Dron

► **To cite this version:**

Muhammad Khalid Salamat, Mohammed M. Moudjou, Jerome Chapuis, Laetitia Herzog, Emilie Jaumain, et al.. Integrity of helix 2-helix 3 domain of the PrP protein is not mandatory for prion replication. *Journal of Biological Chemistry*, 2012, 287 (23), pp.18953-18964. 10.1074/jbc.M112.341677 . hal-02651239

HAL Id: hal-02651239

<https://hal.inrae.fr/hal-02651239>

Submitted on 29 May 2020

HAL is a multi-disciplinary open access archive for the deposit and dissemination of scientific research documents, whether they are published or not. The documents may come from teaching and research institutions in France or abroad, or from public or private research centers.

L'archive ouverte pluridisciplinaire **HAL**, est destinée au dépôt et à la diffusion de documents scientifiques de niveau recherche, publiés ou non, émanant des établissements d'enseignement et de recherche français ou étrangers, des laboratoires publics ou privés.

Integrity of Helix 2-Helix 3 Domain of the PrP Protein Is Not Mandatory for Prion Replication*[§]

Received for publication, January 11, 2012, and in revised form, April 11, 2012. Published, JBC Papers in Press, April 16, 2012, DOI 10.1074/jbc.M112.341677

Khalid Salamat^{†1}, Mohammed Moudjou[‡], Jérôme Chapuis[‡], Laetitia Herzog[‡], Emilie Jaumain[‡], Vincent Béringue[‡], Human Rezaei[‡], Annalisa Pastore[§], Hubert Laude[‡], and Michel Dron^{‡2}

From the [†]INRA, UR892 Virologie Immunologie Moléculaires, F-78350 Jouy-en-Josas, France and the [§]MRC National Institute for Medical Research, The Ridgeway, London NW7 1AA, United Kingdom

Background: Prions are self-propagating β -sheet-rich conformers of PrP protein, however, domains involved in conformational modification remain undetermined.

Results: Peptide insertions in the H2-H3 inter-helix segment or C-terminal part of H2 do not prevent prion replication.

Conclusion: The center of the H2-H3 domain of PrP is not critical for prion conversion.

Significance: These data improve current knowledge on structural features of prions.

The process of prion conversion is not yet well understood at the molecular level. The regions critical for the conformational change of PrP remain mostly debated and the extent of sequence change acceptable for prion conversion is poorly documented. To achieve progress on these issues, we applied a reverse genetic approach using the Rov cell system. This allowed us to test the susceptibility of a number of insertion mutants to conversion into prion in the absence of wild-type PrP molecules. We were able to propagate several prions with 8 to 16 extra amino acids, including a polyglycine stretch and His or FLAG tags, inserted in the middle of the protease-resistant fragment. These results demonstrate the possibility to increase the length of the loop between helices H2 and H3 up to 4-fold, without preventing prion replication. They also indicate that this loop probably remains unstructured in PrP^{Sc}. We also showed that *bona fide* prions can be produced following insertion of octapeptides in the two C-terminal turns of H2. These insertions do not interfere with the overall fold of the H2-H3 domain indicating that the highly conserved sequence of the terminal part of H2 is not critical for the conversion. Altogether these data showed that the amplitude of modifications acceptable for prion conversion in the core of the globular domain of PrP is much greater than one might have assumed. These observations should help to refine structural models of PrP^{Sc} and elucidate the conformational changes underlying prions generation.

Prions cause fatal neurodegenerative diseases such as Creutzfeldt-Jakob disease, Gerstmann-Straussler-Scheinker syndrome, and fatal familial insomnia in humans, scrapie in sheep and goats, bovine spongiform encephalopathy in cattle, and chronic wasting disease in cervids. These disorders are associated with the conformational conversion of a monomeric

cellular prion protein, PrP^C,³ to an aggregated, pathological form, PrP^{Sc} (1, 2). Although the structure of PrP^C is well characterized (3–5), that of the abnormally folded conformer PrP^{Sc} remains a critical challenge. PrP^C is a conserved cell surface, GPI-anchored glycoprotein that comprises an unstructured NH₂-proximal half followed by a globular part arranged in three α -helices and a short antiparallel β -pleated sheet. A single disulfide bond keeps helices 2 and 3 closely arranged. Although PrP^C and PrP^{Sc} appear to have identical primary structures, they differ profoundly in secondary structure and biophysical properties. PrP^C is largely helical and sensitive to proteinase K (PK) digestion, whereas PrP^{Sc} is enriched in β -structure, insoluble, and partially resistant to PK (6–11). The conformational dynamic changes underlying PrP^{Sc} formation remain enigmatic, as well as the structural features conferring PK resistance to the infectivity associated, prion protein core, usually starting at residue ~82–97 and extending up to the C terminus (12–15). There is evidential consensus that the N-terminal moiety, removed by PK treatment *in vitro* or lysosomal proteases in cells (16, 17), is not essential for the replication because prions were generated from the N-terminal-deleted PrP (either Δ 23–88 or Δ 32–93) in infected transgenic mice (18, 19). Decisive experimental data about which region of the PrP PK-resistant domain carries the information for structural transition are still lacking, yet a number of theoretical models have been proposed. Some models consider either the N- (20, 21) or C-terminal part (22–25) of the PK-resistant domain as the minimum essential region that supports structural modifications, whereas others involve both parts of the PK-resistant domain as being essential for prion conversion (11, 26). It is worth noting that the punctual missense mutations associated with inherited forms of prion diseases are clustered between residues 97 and 148 and between 178 and 238 (27). Reverse genetic approaches to express modified PrP sequences have provided some clues but are constrained by the fact that mini-

* This work was supported by the Institut National de la Recherche Agronomique (INRA).

[§] This article contains supplemental Table S1 and Figs. S1–S5.

¹ Supported by the Higher Education Commission of Pakistan and the INRA Animal Health division.

² To whom correspondence should be addressed. Tel.: 33-1-34652611; Fax: 33-1-34652621; E-mail: michel.dron@jouy.inra.fr.

³ The abbreviations used are: PrP^C, normal prion protein; PrP, prion protein; PrP^{Sc}, scrapie-associated PrP; PK, proteinase K; PrP^{res}, PK-resistant PrP^{Sc}; IMAC, immobilized metal affinity chromatography; HSQC, heteronuclear single quantum coherence; PNGase, peptide:N-glycosidase; BisTris, 2-[bis(2-hydroxyethyl)amino]-2-(hydroxymethyl)propane-1,3-diol.

Prions with Insertions in the H2-H3 Domain

mal amino acid substitutions in the PrP protein can hamper prion replication and/or may have a dramatic effect on the susceptibility to infection (28–31). Deletions within the protease-resistant domain, whereas inducing neuropathology (32–35), generally do not allow prion replication, except for PrP106, *i.e.* PrP with two deletions (Δ 23–88, Δ 141–176), the so called miniprion (18). However, subsequent studies led these authors to propose the participation of the 141–176 region in the structural changes (20). Recently Myc or tetracysteine tags were introduced by insertion or sequence modification at one each end of the PK-resistant domain (36–38), and shown to be compatible with prion conversion. However, introduction of such tags farther within this domain had so far prevented prion replication (36, 38). Here we report the conversion into prion of several PrP mutants with an insertion of 8–16 amino acids in the middle of the H2-H3 region, hence demonstrating an unexpected tolerance to sequence modification in a central part of the PK-resistant core.

EXPERIMENTAL PROCEDURES

Ethic Statement—All animal experiments have been performed in accordance with the European Community Council directive 86/609/EEC.

Generation of PrP Insertion Mutants—Insertions and substitutions were introduced by site-directed mutagenesis (QuikChange II mutagenesis kit, Stratagene) into sheep PrP (allotype Val¹³⁶-Arg¹⁵⁴-Gln¹⁷¹) cloned into pTRE plasmid (Clontech) using mutagenic primers (supplemental Table S1). The plasmid encoding PrP-ins203, *i.e.* with an in-frame insertion of 24 bp, was isolated during screening of an experiment originally intended to modify the second site of glycosylation (31). The sequences of all the mutant constructs were verified by sequencing. Numbers indicated for each insertion refer to the position of the first amino acid of the insert according to the sheep PrP numbering.

Cell Culture and Isolation of Rov Cells—Rov cells are epithelial RK13 cells that stably express either wild-type (WT) or mutant ovine PrP using a tetracycline-inducible system (31, 39). They were obtained by transfection and puromycin selection and were grown in Opti-MEM medium (Invitrogen) supplemented with 10% fetal calf serum (FCS) and antibiotics, and split at 1:4 after trypsin dissociation once a week. To assess PrP^C expression, cells were cultivated in the continuous presence of 1 μ g/ml of doxycycline (Sigma).

Antibodies—Several mouse anti-PrP monoclonal antibodies (mAb) were used. The 4F2 mAb (40) is an IgG2b directed to the octarepeat domain (54–92, sheep PrP numbering) and was used to detect PrP^C; Sha31 mAb (epitope 148–159) (40) was used to detect PrP^{res} on immunoblots. The V14 mAb (IgG2a) recognizes a conformational epitope (191–199), sensitive to the presence of *N*-glycan chains (5, 41). ICSM33 (IgG2b, epitope 91–110, D-Gen Ltd., London) was used to detect denatured PrP^{Sc} by immunofluorescence (42). 12F10 (IgG2a epitope 142–160, (43) was used for PrP^{res} detection on histoblots. The anti-FLAG M2 mAb was from Sigma. Alexa Fluor (either 468 or 568) conjugated goat anti-mouse IgG, IgG1, IgG2a, and IgG2b were purchased from Molecular Probes and were all used at a 1/500 dilution.

Prion Infection of Cell Cultures—Rov cells were infected with the cloned 127S scrapie strain as previously described (31) using 1% (w/v) brain pool homogenates of terminally ill *tg338* mice (44). Two days postexposure cells were washed, incubated for 2 additional days, trypsinized, and split at 1:10 dilution. Cells were further incubated for 1 week before analysis (passage 1) and split at 1:4 dilution at each following passage. To test the infectivity of cultures propagating mutant PrP^{Sc} cells were harvested at passage 6–8 postexposure, pelleted, frozen and thawed, then sonicated, and used as inoculums.

Cell Lysis, Proteinase K Digestion, and PNGase Treatment—Cells were washed twice with cold phosphate-buffered saline and whole cell lysates were prepared at 4 °C in TL1 buffer (50 mM Tris-HCl, pH 7.4, 0.5% sodium deoxycholate, 0.5% Triton X-100). Lysates were clarified by centrifugation for 2 min at 800 \times *g* and protein concentrations were determined by microBCA assay (Pierce). For PrP^{res}, lysates were incubated with 4 μ g of PK per 1 mg of protein, for 2 h at 37 °C, then centrifuged for 30 min at 22,000 \times *g*. Pellets were dissolved in Laemmli sample buffer and boiled for 5 min at 100 °C. When needed, 500 units of PNGase F (New England Biolabs, MA) and 1% Nonidet P-40 were added to denatured proteins that were further incubated at 37 °C (17).

Transgenic Mice, in Vivo Infections, and Tissue Homogenate Preparation—To test for the infectivity of PrP^{Sc}-ins203, 5 \times 10⁶ Rov-ins203 or RK13 cells were harvested by scraping at passage 8 post-infection. Cell pellets were resuspended in 100 μ l of medium containing 5% glucose and antibiotics, then frozen and thawed three times before sonication for 1 min. A 20- μ l aliquot of these cellular lysates was injected intracranially to *tg338* mice overexpressing the VRQ allele of ovine PrP (44). Brains and spleens of infected animals were harvested at the terminal stage of the disease and analyzed for PrP^{res} content and distribution by immunoblots and histoblots, respectively, as described previously (45).

Immunoblotting Detection of PrP^C and PrP^{res}—Either 12 or 4–12% NuPage BisTris polyacrylamide gels (Invitrogen) were used for SDS-PAGE. For PrP^C analysis, 50 μ g of protein were deposited on the gel. For PrP^{res}, samples corresponding to the PK-resistant PrP present in 50 μ g of protein of the cellular lysate were loaded on the gel, except for PrP^{res}-ins(Gly₆) and PrP^{res}-ins(FLAG), which an equivalent of 250 μ g of protein were loaded as indicated in the figure legends (Figs. 4D and 5D). The transfer of proteins, their detection and revelation were described previously (17).

Conformational Stability Assay—Cellular lysates were brought to the desired concentration of guanidine HCl, incubated for 1 h at 20 °C under agitation, then diluted to reach the same volume and guanidine HCl concentration (800 μ l, 0.5 M). 200 μ l of 5 \times digestion buffer (750 mM Tris-HCl, pH 7.4, 10% Sarkosyl and 20 μ g/ml of PK) was added and samples were incubated for 1 h at 37 °C under agitation, before methanol precipitation and analysis by immunoblotting.

Cu²⁺-Immobilized Metal Affinity Chromatography (IMAC) Hitrap Chromatography—The AKTA Purifier100 FPLC chromatographic system was used (GE Healthcare) as previously described (17, 46). One milliliter of cell lysates (1 mg of protein) made in TNT buffer (50 mM Tris-HCl, pH 7.4, 150 mM NaCl,

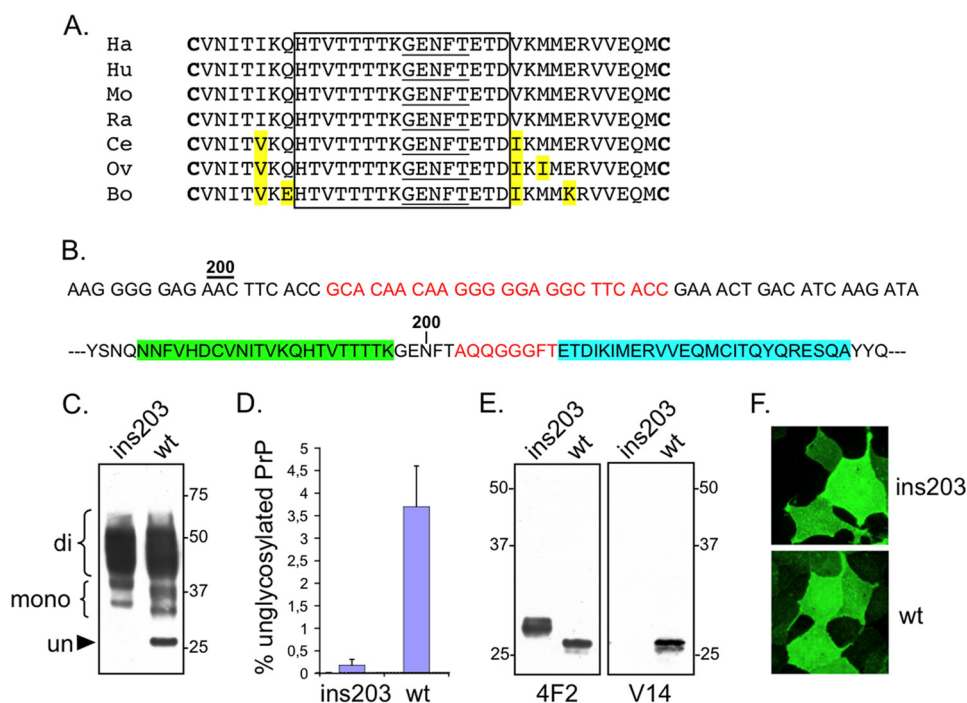


FIGURE 1. Characteristics of a PrP with 8 amino acids inserted in front of helix-3. *A*, the sequences of mammalian PrP included between the 2 cysteines are highly conserved. Identical amino acids are boxed and those corresponding to the H2-H3 loop are underlined. *B*, nucleotide (top line) and primary sequences of PrP-ins203. In this and subsequent figures, the insert is in red and helices H2 and H3 are highlighted in green and blue, respectively. The asparagine of the second site of glycosylation is marked. *C*, glycoforms profiles of WT PrP and PrP-ins203 as shown by immunoblotting (mAb 4F2). Molecular masses markers (in kDa) are indicated. *D*, ratios of the unglycosylated form as quantified from four immunoblots. *E*, PNGase treatment of samples showing the lower mobility of deglycosylated PrP-ins203 compared with WT PrP on a resolutive gel (left, 4F2 mAb). Analysis of a similar blot with the V14 mAb reveals only the WT PrP (right). *F*, immunofluorescence with anti-PrP antibody shows a similar cell surface expression of the WT and mutant protein (4F2 mAb).

and 1% Triton X-100) supplemented with protease inhibitors (Roche Applied Science) was injected into the column. Columns were washed and a linear gradient of 3–200 mM imidazole in TNT buffer was applied to elute column-bound proteins at a flow rate of 1 ml/min for 10 min; 0.5-ml fractions were collected. To solubilize aggregates of PrP^{Sc}-ins(His₆), all buffers were complemented with 4 M urea. Eluted fractions were either treated with 5 μg/ml of PK and precipitated with cold methanol after addition of 20 μg of BSA as a protein carrier or methanol precipitated without PK treatment for total PrP. Individual columns were dedicated to each type of lysate.

Immunofluorescence—Cells were fixed with 4% paraformaldehyde and PrP^C was detected as previously described (31, 47). For PrP^{Sc} immunodetection, fixed and permeabilized cells were treated for 5 min with 3.5 M guanidium thiocyanate and washed three times before exposure to ICSM33 mAb as previously described (42, 47), or to both ICSM33 and M2 anti-FLAG mAbs and then to fluorescent anti-IgG2b and anti-IgG1. Images were acquired with an Axio observer Z1 microscope (Zeiss) and a coolsnap HQ² camera (Photometrics) driven by the Axiovision imaging system software.

NMR Measurements—Recombinant proteins (WT PrP, PrP-ins191, and PrP-ins193) were produced and purified from *Escherichia coli* as published previously (25). HSQC experiments were run at 25 °C on 0.5–0.7 mM ¹⁵N-labeled samples of wild-type PrP and mutants using a VARIAN INOVA 600 MHz. The samples were in 5 mM MOPS buffer, pH 7.0. Water suppression was achieved with a standard Watagate pulse sequence.

Circular Dichroism—CD measurements were carried out on a Jasco-715 spectropolarimeter equipped with a thermostated

cell holder controlled by a Jasco Peltier element. Far-UV CD spectra were recorded from 260 to 195 nm at 25 °C in a 1-mm path-length quartz cuvette at a protein concentration of 12 μM in 5 mM MOPS buffer, pH 7.0. Each CD spectrum was obtained by averaging 15 scans collected at a scan rate of 200 nm/min. Baseline spectra obtained with buffer were subtracted for all spectra. The thermal denaturation scans were obtained by heating a 12 μM sample from 20 to 97 °C at 2 °C/min and by monitoring the ellipticity at 220 nm with a 4-s averaging time and a 0.2 °C data pitch. The thermogram was analyzed assuming a two-state model.

RESULTS

PrP^C with Extended H2-H3 Loop Can Convert into Prion—In a previous study aimed at producing PrP glycosylation mutants (31), we identified a mutant that contained an insertion of 8 amino acids downstream from the second glycosylation site, within the unstructured loop joining helices H2 and H3 of sheep PrP (Fig. 1, A and B). This mutant, denoted PrP-ins203, arose fortuitously probably due to a misalignment of the mutagenic primers used. To examine the effects of this mutation on PrP glycosylation and permissiveness to prion infection, PrP-ins203 was stably expressed in RK13 cells. Immunoblotting analysis revealed the presence of mono- and diglycosylated PrP-ins203 but the apparent lack of the unglycosylated form (Fig. 1C). By quantification on overexposed blots, this latter form was found to be 15–20-fold less abundant than WT PrP (Fig. 1D). PrP-ins203 polypeptide showed a slightly reduced mobility compared with WT PrP, consistent with the presence of additional residues (Fig. 1E). The anti-PrP mAb V14, which

Prions with Insertions in the H2-H3 Domain

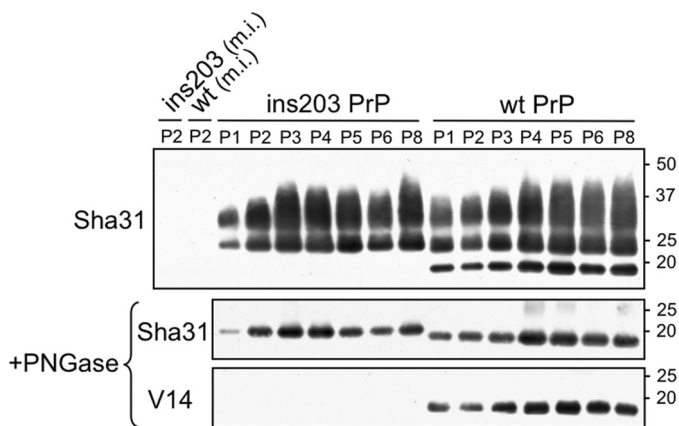


FIGURE 2. 127S-infected Rov-ins203 cells produce self-propagating PrP^{res}. Infected cell cultures were split once a week and samples of PK-digested cellular lysates were analyzed by immunoblotting, the passage number is indicated at the top of the upper panel. Note that the unglycosylated form of PrP^{Sc}-ins203 was not detected to this level of exposure and that, as expected, mock-infected cells (*m.i.*) did not produce protease-resistant PrP. In the lower two panels, PrP^{res} was treated with PNGase F before immunoblotting. Sha31 anti-PrP antibody recognizes an epitope located in the helix H1, whereas V14 antibody recognizes a conformational epitope previously localized nearby and upstream of the insert.

recognizes a conformational epitope (amino acids 191–199) encompassing a region located nearby upstream of the site of insertion of the octapeptide ins-203 (5, 41), was unable to recognize PrP-ins203 (Fig. 1E and supplemental Fig. S1). This suggested that the presence of additional amino acids just downstream of the V14 epitope somehow modifies the local conformation of the PrP. Yet the insertion mutant was correctly routed to the cell surface, as ascertained by PrP immunofluorescence labeling of intact cells (Fig. 1F) and presence in lipid rafts (supplemental Fig. S2).

Cells expressing either WT or mutant PrP were infected with the 127S strain of ovine prion and analyzed for their PrP^{res} content at subsequent passages of cultures. The immunoblot in Fig. 2 shows that PrP-ins203 was converted into a self-propagating, protease-resistant species with amounts of PrP^{res} comparable with those in cells expressing WT PrP (Fig. 2). After PNGase treatment, the PrP^{res} fragment of the insertion mutant was shown slightly bigger in size than WT PrP, thus indicating that the inserted amino acid stretch was protected from protease digestion in PrP^{Sc}. To further characterize the PrP-ins203 mutant we subjected it to a conformational stability assay using guanidine hydrochloride as a denaturing agent (48). The insertion did not appreciably modify the resistance to denaturation (Fig. 3A), because half-denaturation of the mutant and WT PrP^{Sc} occurred at 1.4 ± 0.2 and 1.3 ± 0.4 M, respectively.

PrP-ins203 conferred cells similar susceptibility to prion infection as WT PrP in cell cultures exposed to serial dilutions of 127S-infected mouse brain homogenate. Both Rov-wt and Rov-ins203 produced large amounts of PrP^{res} after exposure to inoculum at the 10^{-3} dilution, whereas no PrP^{res} was detected beyond the 10^{-4} dilution (Fig. 3B). To confirm that PrP-ins203 led to the generation of infectious prion, the cell homogenate from 8 passages on Rov-ins203 cultures was inoculated to naive Rov-ins203 or Rov-wt cells, and to *tg338* mice. Both homotypic and allotypic cell cultures were successfully infected based on PrP^{res} accumulation (Fig. 3C). Mice inoculated with the PrP-

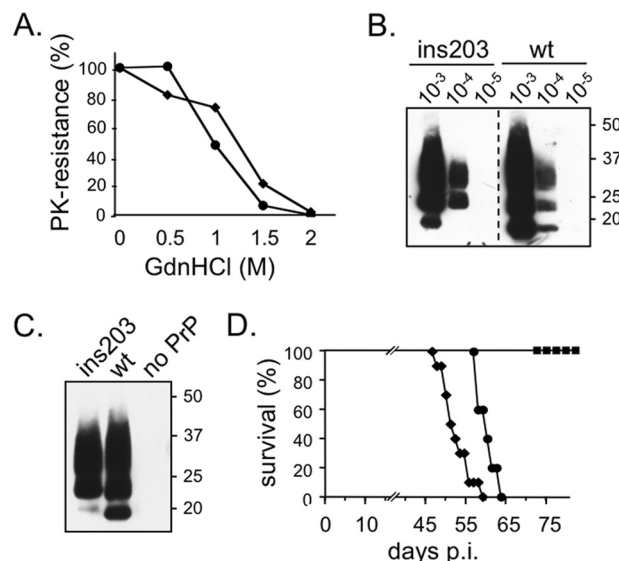


FIGURE 3. PrP-ins203 is as susceptible as WT PrP to prion infection and PrP^{Sc}-ins203 is infectious. A, WT and ins203 PrP^{res} have a similar sensitivity to guanidine denaturation. A representative experiment of the conformational stability assay shows that resistance to PK digestion of PrP^{res} after denaturation by increasing guanidium chloride concentrations was not appreciably modified for PrP^{res}-ins203 (●) compared with WT PrP^{res} (◆). B, PrP-ins203 has the same susceptibility to prion infection as WT PrP. A 10% (w/v) brain homogenate from 127S-infected mice was diluted and used to infect cells expressing either WT or ins203 PrP as indicated at the top of the panel. The PrP^{res} content was determined at the third passage of the cultures post-infection. C, *de novo* infection of Rov (*wt*), RK13 (*no PrP*), and Rov-ins203 cells by PrP^{Sc}-ins203. A cellular homogenate of Rov-ins203 cells at passage number six post-infection was used as inoculum for *de novo* infections. D, PrP^{Sc}-ins203 inoculum killed mice in 2 months. The curves show the survival rate of *tg338* mice challenged by intracranial inoculation of homogenates from either 127S-infected Rov-ins203 cells at passage eight (●) or brains of terminally ill mice (◆). All mice (5/5) inoculated with control homogenate from 127S-infected RK13 cells, which do not express PrP, grown in parallel with Rov-ins203, stayed healthy (■).

ins203-derived homogenate died at 61 ± 2 days with typical TSE signs (Fig. 3D) and showed the presence of PrP^{res} with a glycoform pattern and regional deposition in the brain typical of the 127S strain (supplemental Fig. S3). Altogether these results demonstrate that a mutant PrP with an 8-amino acid insertion in the PK-resistant core is efficiently convertible into *bona fide* prion.

Insertion of Glycine Residues, or Extension of the H2-H3 Loop Up to 16 Amino Acids Do Not Prevent Prion Replication—We modified the original insertion already containing 3 glycine residues to create a segment containing 6 glycines (Fig. 4A). Because a feature of the polyglycine stretch is to be incompatible with the formation of secondary, either α -helix or β -sheet structures, it was assumed that the insert ins203(Gly₆) would neither participate to elongation of H3 nor convert into a β -sheet segment if PrP^{Sc} were to be produced. When expressed in cells, PrP-ins203(Gly₆) showed a glycoform pattern with a low level of the unglycosylated form as for the original PrP-ins203, and some decrease in the proportion of the diglycosylated form (Fig. 4B). PrP-ins203(Gly₆) was efficiently routed to the cell surface and found to be associated with lipid raft fractions (supplemental Fig. S2) and was converted into PK-resistant species upon infection with 127S prion (Fig. 4, C and D). PrP^{Sc}-ins203(Gly₆) was readily propagated along with five sub-passages, although the amount of PrP^{res} was reduced by at least

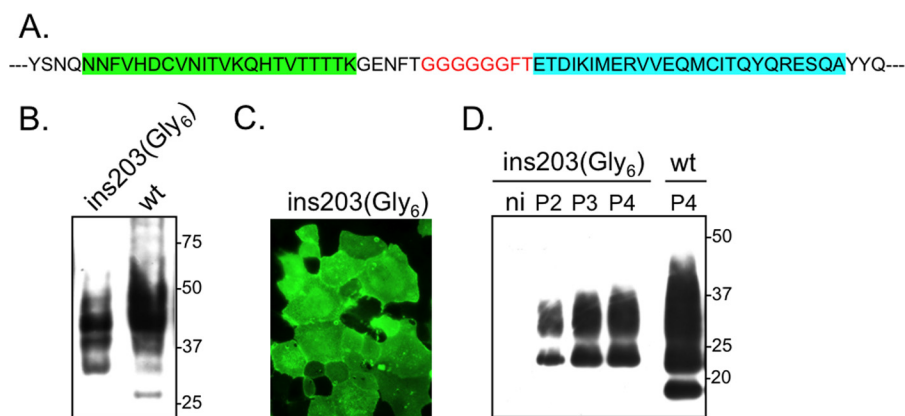


FIGURE 4. **PrP-ins203(Gly₆) is convertible into prion.** *A*, amino acid sequence of the mutated region of PrP-ins203(Gly₆). *B*, immunoblot showing that the unglycosylated species are markedly under-represented for the insertion mutant compared with WT PrP. (4F2 mAb). *C*, immunofluorescence with anti-PrP antibodies showing that the insertion mutant is properly routed to the cell surface (4F2mAb). *D*, Western blot analysis of PK-treated samples. The gel was loaded with 250 or 50 μ g of PK-digested protein for the mutant PrP and WT PrP, respectively. PrP containing the polyglycine stretch was successfully converted into a self-propagating PK-resistant protein but levels of PrP^{res} accumulated in cells were lower than for the WT PrP (Sha31 mAb).

10-fold compared with that in WT PrP Rov cells (Fig. 4D). Thus, extension of the loop between H2 and H3 by a polyglycine stretch remained compatible with PrP^{Sc} formation, suggesting that this part of the protein is unstructured in misfolded conformers.

We also introduced an 8-amino acid FLAG sequence into the original ins203 octapeptide, enabling us to recognize the presence of the insert using a relevant antibody (Fig. 5A). As for other ins203 insertions, the unglycosylated forms of PrP-ins(FLAG) were produced in low amounts in RK13 cells (Fig. 5B), and FLAG-PrP was efficiently expressed at the cell surface (Fig. 5C). Rov-ins203(FLAG) were susceptible to prion infection and generated self-propagating PrP^{Sc}, however, the PrP^{res} levels were markedly reduced compared with WT PrP (Fig. 5D). Cells in which PrP^{Sc} had accumulated efficiently exhibited numerous aggregates labeled, after guanidium thiocyanate denaturation, by anti-PrP and anti-FLAG antibodies (Fig. 5E). We further showed that PrP^{Sc}-ins(FLAG) autopropagated in cell culture was also infectious for Rov-wt cells (Fig. 5F). Altogether these results established that a PrP^C with a 4-fold increase, *i.e.* from 5 to 21 amino acids, of the size of the sequence between H2 and H3 can be converted into *bona fide* prions.

Production of His-tagged PrP^{Sc}—As a means to facilitate PrP purification, the first 6 amino acids of ins203 were substituted by histidine residues and the resulting PrP-ins203(His₆) was expressed in RK13 cells (Fig. 6A). The functionality of the tag was tested by loading cellular lysates onto Cu²⁺-IMAC columns. Because PrP already contains an N-terminal octarepeat sequence, a strong binding site for divalent ions, both WT and the His-tag PrP^C were retained on such columns (Fig. 6B). However, PrP-ins(His₆) was eluted at a much higher concentration of the Cu²⁺ competitor imidazole (150 mM) than WT PrP (90 mM), indicating that the His tag actually increased the avidity for immobilized copper ions of PrP (Fig. 6C), including diglycosylated molecules where complex *N*-glycan chains are attached close to the tag. Interestingly, the fractions in which His tag PrP was eluted contained at least 10-fold less contaminant proteins than the fractions containing WT PrP (not shown).

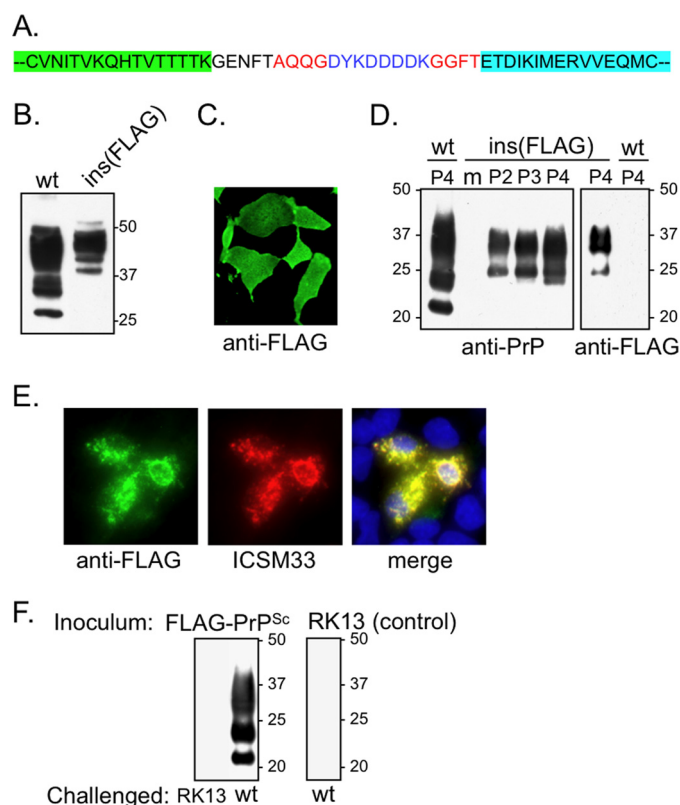


FIGURE 5. **PrP-ins203(FLAG) with a H2-H3 loop extended by 16 additional amino acids is convertible into a true prion.** *A*, primary sequence of the FLAG-tagged mutant PrP. The FLAG sequence (*blue*) was inserted in the middle of the original ins203 sequence (*red*). *B*, analysis of Rov-ins203(FLAG) expression by immunoblotting (4F2 mAb). *C*, cell surface expression of PrP-ins203(FLAG) on nonpermeabilized cells. *D*, PrP^{res} detection by immunoblot (*left panel*, Sha31 mAb) for infected and mock-infected (*m*) cells. The gel was loaded with 250 or 50 μ g of PK-digested protein for the mutant PrP and the WT PrP, respectively. Presence of the FLAG was verified by a specific antibody (*right panel*). *E*, detection of PrP^{Sc} by immunofluorescence. Prion-infected Rov-ins203(FLAG) cells were immunolabeled by anti-PrP and anti-FLAG antibodies. Merge images with nuclei labeled by DAPI (*blue*) showed colocalization of PrP^{Sc} and FLAG signals in infected cells (*yellow*). *F*, *de novo* infection of WT Rov cells challenged with homogenate from Rov-ins203(FLAG) cells propagating a PrP^{Sc} for five passages. The third passage post-infection is shown (*left panel*). RK13 cells infected by 1275 brain homogenate at the same time and maintained in the same conditions as Rov-ins203(FLAG) were used to control the absence of residual infectious brain material in the culture (*right panel*).

Prions with Insertions in the H2-H3 Domain

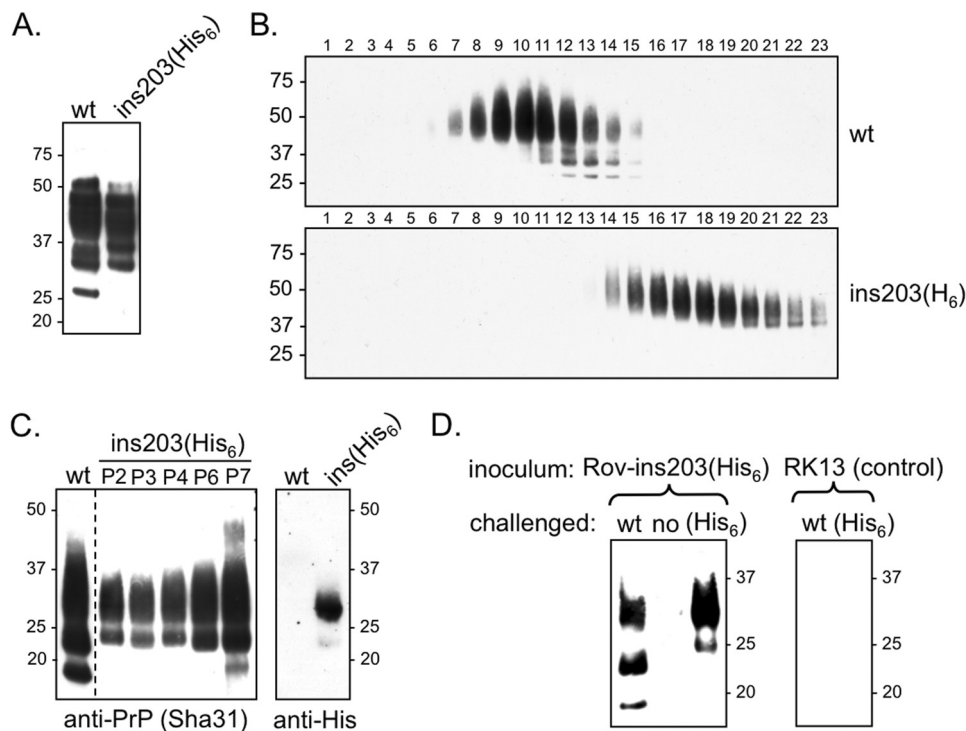


FIGURE 6. Insertion of six histidines increased the copper affinity of PrP^C and PrP-ins(His₆) was converted into a His-tagged prion. *A*, the glycoform pattern of PrP-ins(His₆) shows a reduction of the unglycosylated form similar to the original ins203 PrP (4F2 mAb). *B*, WT PrP was eluted from the Cu²⁺ IMAC column at a lower concentration of imidazole than PrP-ins(His₆). Note that the monoglycosylated forms were eluted after the diglycosylated ones for both WT and ins203(His₆) PrP. Immunoblots were revealed with the 4F2 mAb. *C*, immunoblot showing that PK-resistant PrP was generated upon infection. The rate of PrP^{res} increased notably after five to six passages of the cell culture (*left panel*, Sha31 mAb). The presence of the His tag on the PK-resistant fragment was ascertained using an anti-His₆ mAb (*right panel*). *D*, Rov cells expressing WT PrP and Rov-ins(His₆) were susceptible to *de novo* infection by cellular homogenate of 127S-infected Rov-ins(His₆) harvested at passage six (PK-treated samples and Sha31 mAb).

To determine whether the H2-H3 segment was accessible to interaction into PrP^{Sc} molecules as well, Rov-ins(His₆) cells were subjected to prion infection. Infected cells produced PrP^{res} from the first passage on, the amount of which increased gradually on subpassaging to reach a level comparable with that produced by Rov-wt after 7–8 passages. His-tag PrP^{Sc} was able to infect cultures expressing homotypic as well as WT PrP sequence (Fig. 6, *C* and *D*). Anti-His antibodies recognized the PK-resistant fragment (Fig. 6*C*, *right panel*). The half-denaturation value of PrP^{Sc}-ins(His₆) in conformational stability assay was 1.3 ± 0.25 M, similar to WT and ins203 PrP^{res} (see above).

We also asked whether a His tag inserted in the PK-resistant core would still bind to copper-immobilized ions. Although we did show binding of the His tag PrP^{Sc} to IMAC Cu²⁺ columns (Fig. 7), the bulk of PrP^{Sc} did not bind and was either excluded in the flow-through (Fig. 7, *top panel*) or retained on the column even after application of imidazole at high concentrations (not shown). To improve the purification of His-tagged PrP^{Sc}, cellular lysates were incubated with 4 M urea prior to application on the columns. Proteins recovered by elution with increasing imidazole concentrations were PK-digested and analyzed by immunoblotting. WT PrP^{Sc}, present in Rov cellular lysates essentially as N-terminal truncated species (17), bound to Cu²⁺ columns with low avidity and started to elute at 40 mM imidazole (Fig. 7, *lower panel*). His-tagged PrP^{res} was eluted at higher concentrations of imidazole, starting at 88 mM (Fig. 7, *middle panel*), indicating that the tag could be functional for the PrP^{res} species under adequate conditions of solubility.

Integrity of C-terminal Part of Helix-2 Is Not Essential for Prion Conversion—To determine how variable the exact location of the 8-amino acid insertion could be, we moved it upstream and downstream of the original position (Fig. 8*A*). The insert was introduced at the other end of the inter helix loop (position 198), or in helix H2 (195 to 187) or helix 3 (207 and 210). These mutants were expressed and efficiently reached the cell surface (supplemental Fig. S4*A*), except PrP-ins210, which was not detectably expressed at the membrane but showed intracellular accumulation, essentially at a juxtannuclear position (supplemental Fig. S4*B*). PrP-ins198 did not confer Rov cells susceptibility to prion infection, indicating that even in the unstructured segment considered, the site of insertion might be critical. Cells expressing H3 mutants, Rov-ins207 and Rov-ins210, were not permissive to the infection, yet the convertibility of PrP-ins210 could not be adequately tested due to impaired trafficking.

In contrast, PrP with insertion into H2, 3 amino acids before the end of the helix (position 195) and then further upstream with 1 amino acid increment up to 193 conferred permissiveness to the cells and led to reproducible and robust infection as attested by the formation of self-propagating PrP^{res} (Fig. 8*B*). Demonstration of the infectivity of each of the three mutant PrP^{Sc} was ascertained by using cellular homogenates to challenge naive Rov-wt and homotypic cells (supplemental Fig. S5). Insertion further upstream markedly affected (PrP-ins192) or even hampered (PrP-ins191 and PrP-ins187) prion replication (Fig. 8*B*). These results showed that insertion of extra amino

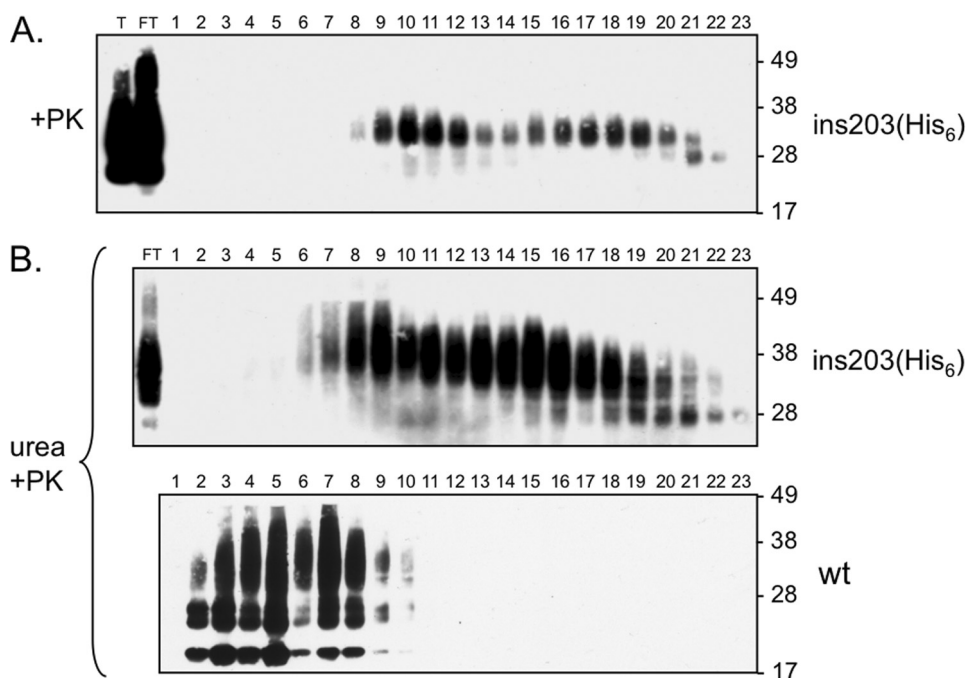


FIGURE 7. **Retention of PrP-ins(His₆) prion by chromatography affinity.** *A*, part of the PK-resistant PrP-ins(His₆) produced by infected cells was retained with high affinity to the column. *B*, PrP^{5C}-ins203(His₆) solubilized with 4 M urea was more efficiently retained on IMAC copper columns than the WT PrP^{res}. At this particular concentration urea allowed complete PK digestion of PrP^C but preserved the protease resistance of both the His tag and WT PrP^{5C}. Eluted samples were treated by PK and analyzed by immunoblotting (Sha31 antibody).

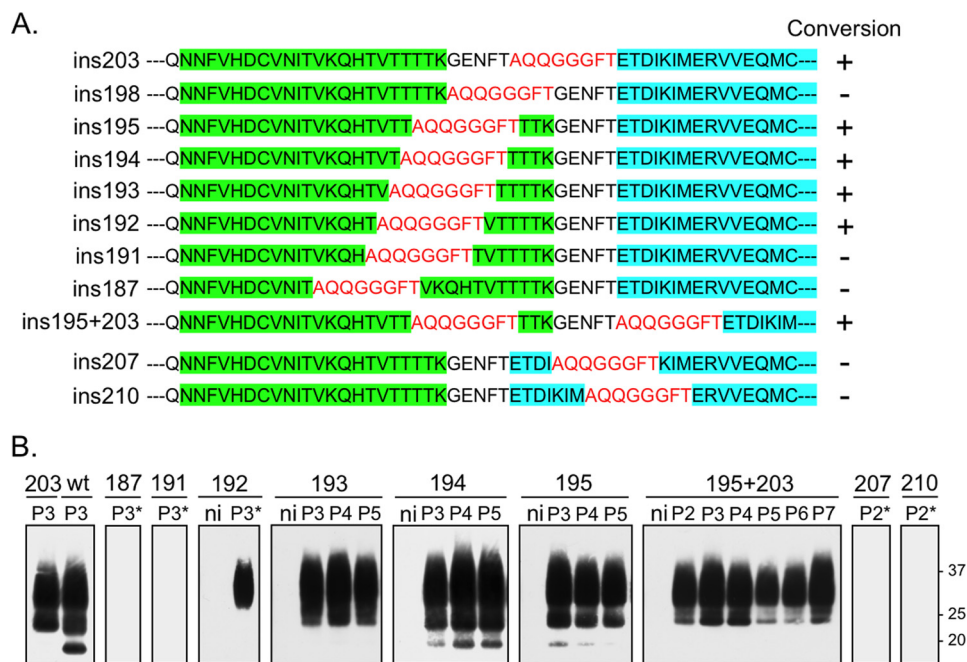


FIGURE 8. **The C-terminal part of helix-2 is not critical for prion conversion.** *A*, sequence of different mutant PrP generated with an insertion located upstream or downstream of the 203 position. The *insert* is in red and amino acids that belong to, or are originally from helix-2 are in green. Note that the bottom sequence contains two inserts, each at a different position. The name of the mutant is on the left and its capacity to convert into prion is indicated on the right. *B*, assay for PrP^{res} content of the insertion mutant PrP modifying the loop, the helices, or both. The same amount of protein digested by PK was used throughout. The passage number is indicated above each panel and the asterisk indicates that a longer exposure is shown.

acids in the part of the protein corresponding to last two turns of H2 (Fig. 9) did not prevent prion formation, whereas introduction of the same insertion further upstream in the helix impaired conversion.

Insertions in H2 C Terminus Do Not Interfere with PrP-fold—To understand whether the inserted sequences affect the fold of

PrP, we recorded NMR ¹⁵N HSQC experiments, which are sensitive to protein tertiary fold. As insertions in H2 could be more destabilizing for mutants than insertion in the loop, we specifically analyzed PrP-ins193 and PrP-ins191. The former is competent for prion conversion but not the latter, although they are both expressed at the cell surface and found associated with

Prions with Insertions in the H2-H3 Domain

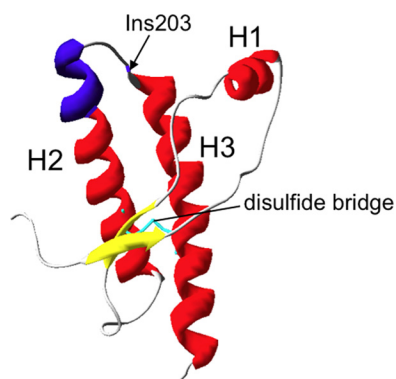


FIGURE 9. Schematic structure of WT PrP with the indication of regions tolerant to insertion. α -Helices are shown in red and the two short β -sheets in yellow. H2 and H3 are linked by a disulfide bond that maintains them close to each other, and the unstructured inter-helix segment forms a loop. The position where the four different insertions (ins203, ins203(Gly₆), ins203(His₆), and ins203(FLAG)) were introduced, just before H3, is indicated. The C-terminal part of H2 in which octapeptides can be introduced without preventing prion conversion is colored in dark blue.

lipid rafts (supplemental Figs. S2 and S4). Moreover the insertion is moved only 2 amino acids toward the center of H2 in the PrP-ins191 with respect to the PrP-ins193. The spectra of the wild-type and mutant proteins were similar (Fig. 10A). They all showed a good resonance spreading that is typical of folded proteins indicating that the insertions do not significantly affect the tertiary structure, which is thus retained. Minor differences can reasonably be attributed to a different packing of the secondary structural elements in the three proteins that leads to different local chemical environments. These results are consistent with previous observations that had proven that the presence of the disulfide bridge in the middle of H2 and H3 is essential for retaining the fold of the core element H2-H3 (25); we do not observe a major destabilization because the insertions introduced do not affect the disulfide bridge.

To understanding further the role of the insertions, which is whether they introduce additional secondary structures by elongating the helices or merely substitute the native structure, we recorded far-UV CD spectra of PrP-ins191 and PrP-ins193 and compared them with that of the wild-type protein (Fig. 10B). They were identical within experimental error suggesting that the additional residues do not promote formation of an additional secondary structure. Finally, we questioned whether the insertions would have an effect on the fold stability. We recorded temperature scans followed by CD. We observed that, whereas having very similar highly cooperative behavior, the wild-type seemed to reproducibly be 2–3 °C more stable than the two mutants suggesting that, if at all, the insertions have a mild destabilizing effect (Fig. 10B). Taken together these results tell us that these insertions do not perturb the overall fold of PrP^C.

Conversion into Prion of Mutant with Two Insertions—We have also constructed a double mutant by inserting the octapeptide concomitantly at two places previously found to be tolerant to insertion, *i.e.* at position 195, into H2, and at position 203, in the loop between H2 and H3. Upon infection, PrP-ins(195 + 203) was convertible into a prion that was readily and reproducibly (3 times out of 3 trials) propagated in cell culture (Fig. 8). Thus again, mutant PrP with 16 additional amino acids in a central part of the PK-resistant core proved to be apt to form prion.

DISCUSSION

In this study, we expressed a number of sheep PrP mutants displaying a peptide insertion at various places and we show that nine mutants with exogenous sequences introduced in the central part of the H2-H3 region remain convertible into prions, thus questioning how critical is the integrity of this region for the conversion into PrP^{Sc}. This issue is important particularly in view of several recent reports proposing the crucial involvement of the H2-H3 region in misfolding events leading to prion formation (11, 22, 24, 26, 49, 50).

PrP Proteins with Extended H2-H3 Interhelix Segment Remain Convertible into Prions—Four PrP mutants were built with insertions at position 203 that increased about 2–4-fold the size of the loop joining H2 and H3. The resulting proteins were glycosylated and properly routed to the cell surface, whereas sharing a notable reduction of unglycosylated PrP species. The latter feature might result from an increased glycosylation efficiency (51) or a reduced stability of this form, or both, as observed for the F198S mutation in human (52–54) and for its equivalent in the sheep sequence, F201S (31), both of which are close to the insertion site. Upon prion infection ins203 mutants produced self-propagating PrP^{Sc} albeit at different levels. The original PrP-ins203 generated as much PrP^{res} as WT PrP, whereas cells expressing the His-tagged PrP had to undergo several passages before reaching similar levels, suggesting an adaptation of the prion strain to this particular substrate or selection of most performing components (55). The other two PrP mutants produced lower quantities of PrP^{res}, which may reflect reduced replication efficiency, or a lower stability of the misfolded protein in the cells. Nevertheless, these insertion mutants of PrP^{Sc} were *de novo* infectious for naive cells or for transgenic mice expressing the sheep PrP. Altogether these results proved that *bona fide* prions could be generated despite a substantial increase in size of the segment separating H2 and H3, the heart of structured PrP^{Sc}. The magnitude of acceptable changes in this region was impressive because not only was the size of the H2-H3 connecting segment increased, but the physicochemical characteristics of the loop were also drastically altered. In PrP-ins(His₆) and PrP-ins(FLAG), in particular, the calculated isoelectric point and charge at pH 7 of the loop segment were markedly modified.

PrP^C and PrP^{Sc} Conformations of Insertion Mutants in Position 203—The loss of the conformational V14 epitope in PrP-ins203 might suggest some local dynamic change of the conformation of the region immediately upstream of the insert (56), as the epitope was reported to cover the domain between the two glycosylation sites, from the middle of H2 to the beginning of the H2-H3 loop (5, 41). However, another possibility is that the size of the segment encompassing the epitope would have been previously underestimated. PrP^{Sc}-ins203 had a similar resistance to guanidium denaturation as WT PrP^{Sc}, suggesting no major structural variation between the two misfolded proteins, despite dramatic under-representation of aglycosylated species in PrP^{Sc}-ins203. Moreover, the strain features in tg338 mice of PrP^{Sc}-ins203 were typical of the 127S strain propagated on WT PrP cultures. Importantly, the introduction of six consecutive glycines in the insert did not preclude prion conversion. This

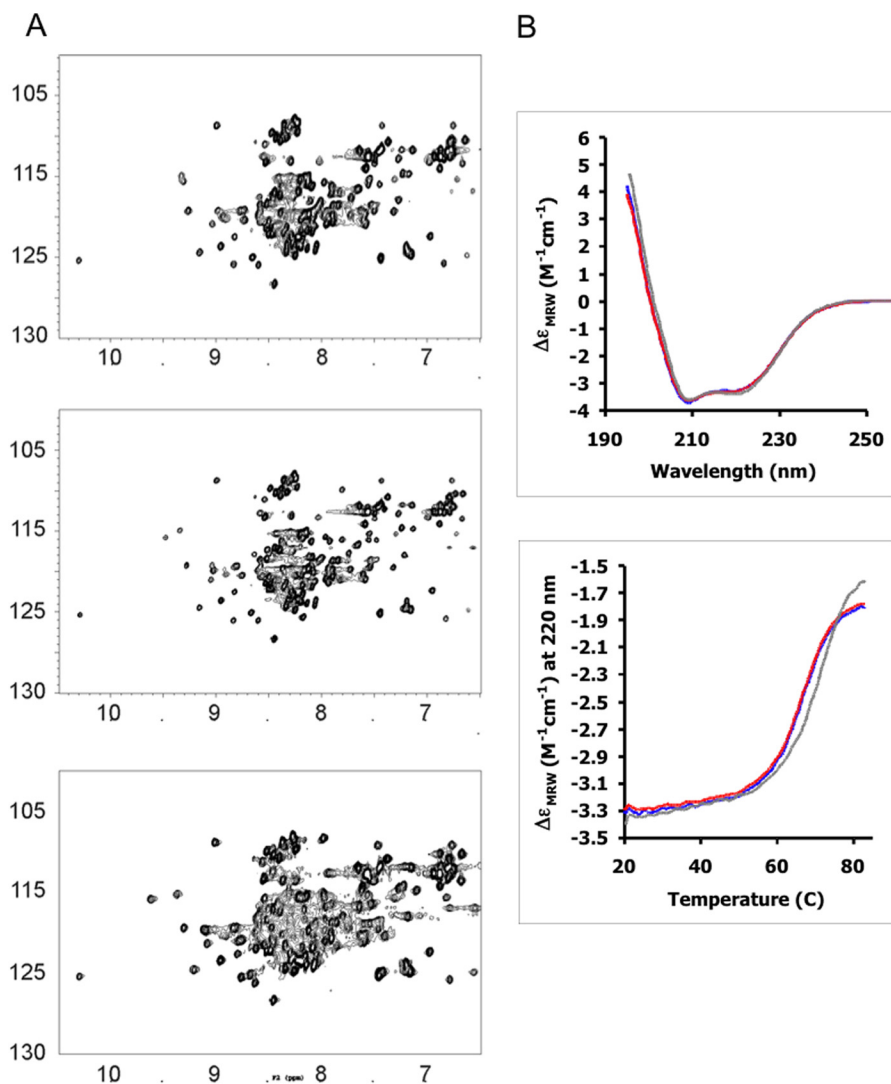


FIGURE 10. **Structural analyses of PrP with insertions in H2 conferring permissiveness to 127S or not.** A, comparison of the NMR HSQC spectra at 25 °C of ins191 (top), ins193 (middle), and wild-type PrP (bottom) recorded at 600 MHz. B, comparison of the far-UV CD (top) and the temperature scans followed at 220 nm (bottom) of ins191 (red), ins193 (blue), and wild-type (black) PrP recorded at 25 °C. The spectra were normalized for the concentration.

finding strongly suggests that the corresponding segment was not changed into the β -sheet in PrP^{Sc}, and comes in support of the structurally based prediction that the loop between H2 and H3 remains unstructured in PrP^{Sc} (20, 22).

Prions Can Be Tagged inside the PK-resistant Core—The insertion of tags might be useful to study the biology of prion infection. Previous observations tended to indicate that the ends of the PK-resistant fragment could be modified, whereas the inside part could not (36–38). In fact, as shown here, tags can be introduced within the protease-resistant segment without blocking prion replication. Despite their location between two heavy *N*-glycan chains, the His tag and FLAG tag were easily accessible in PrP^C and proved to be useful for purification and immunodetection experiments. Yet, purification or detection of His-tagged PrP^{Sc} could not be achieved without partial solubilization of aggregates by urea. Also, PrP^{Sc}-ins(FLAG) was not recognized by anti-FLAG antibodies without prior guanidine treatment of the cells. Both results are consistent with previous observations on other tagged PrP^{Sc} and the inaccessibility of all these tags to proteolytic enzymes in misfolded PrP (36–38).

Integrity of the Last Two Turns of H2 Is Not Mandatory for Prion Replication—Insertion of the octapeptide (AQQGGGFT) either at the beginning of the H2-H3 loop (position 198) and in the N-terminal part of H3 (position 207) impaired the formation of prion. Nevertheless, the integrity of the extremity of H3 or of the first residue of the H2-H3 loop is unlikely to be essential for prion conversion because insertion of another sequence at close proximity appeared to be compatible with PrP^{res} formation (57). In contrast, introduction of the octapeptide in the C-terminal part of H2 allowed the generation of four PrP mutants that all remained prion-compatible as attested by self-propagation of PrP^{res} and *de novo* infectivity of the mutant PrP^{Sc}. Of note, the levels of newly formed PrP^{res} decreased while moving the insertion from position 195 to 192, with no conversion occurring beyond this position. As the thread of helix comprises a little more than 3 amino acids, it means that insertion in the last two C-terminal turns of H2 allowed the formation of *bona fide* prions.

Furthermore, a double mutant with an insert in the last turn of H2 and another in the H2-H3 loop was competent for prion

Prions with Insertions in the H2-H3 Domain

conversion and propagation, showing that the simultaneous modification of both regions was tolerated. Like the PrP-ins-(FLAG) mutant mentioned above, PrP-ins(195 + 203) harbors 16 additional amino acids, strengthening the view that neither the size of the middle part of the H2-H3 region nor the amino acid sequence are critical for 127S prion replication. Altogether these findings were unexpected as the H2-H3 region is proposed to be essential for prion conversion according to several, recently published models (22, 26, 49), in which these two helices are proposed to undergo drastic conformational change and to adopt a β -sheet conformation in the prion state (11, 23, 50). Other models, however, consider that it is mainly the N-terminal moiety of the PK-resistant fragment that supports structural modification (20, 21, 58). Also, a recent paper has reported productive infection in cell cultures expressing a PrP molecule with two point mutations substituting original amino acids by cysteines, one in the H2 end and the other in the loop (59).

Insertions in H2 End Preserve Overall Fold of the H2-H3 Domain—We wonder whether the insertions could have destabilizing effects on the structure of PrP^C and particularly on the H2-H3 domain. This question concerned both the PrP construct competent for prion conversion and those that are not. We thus turned to structural analysis of the recombinant insertion mutant PrP assuming that their structures would reflect characteristics of the corresponding glycosylated PrP anchored at the membrane of mammalian cells. The conclusions from these works that insertions ins193 are compatible with prion conversion and ins191, are not compatible, do not induce significant alteration of the overall fold of PrP.

As a whole, if we assume the increasingly supported hypothesis of a conformational change of the H2-H3 domain in prions (22–26), the comparison of infection data with structural analysis of PrP-ins193 and PrP-ins191 may suggest that when approaching the disulfide bridge, which could induce specific constraints to surrounding areas, modifications of H2 are less important for the overall fold of PrP^C than for its conversion into PrP^{Sc}.

In conclusion we showed that it is possible to generate *bona fide* prions with 8–16 additional amino acids inserted in the middle of the PK-resistant domain, revealing an unexpected tolerance to PrP sequence change in the prion core. More specifically we showed that octapeptide insertions in either the H2-H3 loop or the last two C-proximal turns of H2 were not critical for prion conversion. These findings indicate that the integrity and sequence specificity of the loop and the two adjacent turns of H2 are not determinant for the structure of PrP^{Sc} and will help to validate and refine structural models.

Acknowledgments—We acknowledge Stéphanie Prigent and Sylvie Noinville (INRA Jouy-en Josas, France), Kris Pauwels and Stephen Martin (NIMR London, UK) for help with recombinant PrP and structural analysis. We also acknowledge Jacques Grassi and Stéphanie Simon (CEA, Saclay, France), Jean-Philippe Deslys (CEA, Fontenay aux Roses, France), Jan P. Langeveld (Central Institute for Animal Disease Control, Lelystad, Netherlands), and John Collinge (MRC Prion Unit, UCL Institute of Neurology, UK), for supply of antibodies. We thank Calum MacKichan for English style editing.

REFERENCES

1. Prusiner, S. B. (1998) Prions. *Proc. Natl. Acad. Sci. U.S.A.* **95**, 13363–13383
2. Büeler, H., Aguzzi, A., Sailer, A., Greiner, R. A., Autenried, P., Aguët, M., and Weissmann, C. (1993) Mice devoid of PrP are resistant to scrapie. *Cell* **73**, 1339–1347
3. Riek, R., Hornemann, S., Wider, G., Billeter, M., Glockshuber, R., and Wüthrich, K. (1996) NMR structure of the mouse prion protein domain PrP(121–231). *Nature* **382**, 180–182
4. Donne, D. G., Viles, J. H., Groth, D., Mehlhorn, I., James, T. L., Cohen, F. E., Prusiner, S. B., Wright, P. E., and Dyson, H. J. (1997) Structure of the recombinant full-length hamster prion protein PrP(29–231). The N terminus is highly flexible. *Proc. Natl. Acad. Sci. U.S.A.* **94**, 13452–13457
5. Eghiaian, F., Grosclaude, J., Lesceu, S., Debey, P., Doublet, B., Tréguer, E., Rezaei, H., and Knossow, M. (2004) Insight into the PrP^C→PrP^{Sc} conversion from the structures of antibody-bound ovine prion scrapie-susceptibility variants. *Proc. Natl. Acad. Sci. U.S.A.* **101**, 10254–10259
6. Caughey, B. W., Dong, A., Bhat, K. S., Ernst, D., Hayes, S. F., and Caughey, W. S. (1991) Secondary structure analysis of the scrapie-associated protein PrP 27–30 in water by infrared spectroscopy. *Biochemistry* **30**, 7672–7680
7. Pan, K. M., Baldwin, M., Nguyen, J., Gasset, M., Serban, A., Groth, D., Mehlhorn, I., Huang, Z., Fletterick, R. J., and Cohen, F. E. (1993) Conversion of α -helices into β -sheets features in the formation of the scrapie prion proteins. *Proc. Natl. Acad. Sci. U.S.A.* **90**, 10962–10966
8. Safar, J., Roller, P. P., Gajdusek, D. C., and Gibbs, C. J. (1993) Conformational transitions, dissociation, and unfolding of scrapie amyloid (prion) protein. *J. Biol. Chem.* **268**, 20276–20284
9. Baron, G. S., Hughson, A. G., Raymond, G. J., Offerdahl, D. K., Barton, K. A., Raymond, L. D., Dorward, D. W., and Caughey, B. (2011) Effect of glycans and the glycosphosphatidylinositol anchor on strain dependent conformations of scrapie prion protein. Improved purifications and infrared spectra. *Biochemistry* **50**, 4479–4490
10. Gong, B., Ramos, A., Vázquez-Fernández, E., Silva, C. J., Alonso, J., Liu, Z., and Requena, J. R. (2011) Probing structural differences between PrP(C) and PrP(Sc) by surface nitration and acetylation. Evidence of a conformational change in the C terminus. *Biochemistry* **50**, 4963–4972
11. Smirnovas, V., Baron, G. S., Offerdahl, D. K., Raymond, G. J., Caughey, B., and Surewicz, W. K. (2011) Structural organization of brain-derived mammalian prions examined by hydrogen-deuterium exchange. *Nat. Struct. Mol. Biol.* **18**, 504–506
12. Stahl, N., Baldwin, M. A., Teplow, D. B., Hood, L., Gibson, B. W., Burlingame, A. L., and Prusiner, S. B. (1993) Structural studies of the scrapie prion protein using mass spectrometry and amino acid sequencing. *Biochemistry* **32**, 1991–2002
13. Howells, L. C., Anderson, S., Coldham, N. G., and Sauer, M. J. (2008) Transmissible spongiform encephalopathy strain-associated diversity of N-terminal proteinase K cleavage sites of PrP(Sc) from scrapie-infected and bovine spongiform encephalopathy-infected mice. *Biomarkers* **13**, 393–412
14. Notari, S., Strammiello, R., Capellari, S., Giese, A., Cescatti, M., Grassi, J., Ghetti, B., Langeveld, J. P., Zou, W. Q., Gambetti, P., Kretzschmar, H. A., and Parchi, P. (2008) Characterization of truncated forms of abnormal prion protein in Creutzfeldt-Jakob disease. *J. Biol. Chem.* **283**, 30557–30565
15. Gielbert, A., Davis, L. A., Sayers, A. R., Hope, J., Gill, A. C., and Sauer, M. J. (2009) High-resolution differentiation of transmissible spongiform encephalopathy strains by quantitative N-terminal amino acid profiling (N-TAAP) of PK-digested abnormal prion protein. *J. Mass Spectrom* **44**, 384–396
16. Caughey, B., Raymond, G. J., Ernst, D., and Race, R. E. (1991) N-terminal truncation of the scrapie-associated form of PrP by lysosomal protease(s). Implications regarding the site of conversion of PrP to the protease-resistant state. *J. Virol.* **65**, 6597–6603
17. Dron, M., Moudjou, M., Chapuis, J., Salamat, M. K., Bernard, J., Cronier, S., Langevin, C., and Laude, H. (2010) Endogenous proteolytic cleavage of disease-associated prion protein to produce C2 fragments is strongly cell- and tissue-dependent. *J. Biol. Chem.* **285**, 10252–10264

18. Supattapone, S., Bosque, P., Muramoto, T., Wille, H., Aagaard, C., Peretz, D., Nguyen, H. O., Heinrich, C., Torchia, M., Safar, J., Cohen, F. E., DeArmond, S. J., Prusiner, S. B., and Scott, M. (1999) Prion protein of 106 residues creates an artificial transmission barrier for prion replication in transgenic mice. *Cell* **96**, 869–878
19. Flechsig, E., Shmerling, D., Hegyi, I., Raeber, A. J., Fischer, M., Cozzio, A., von Mering, C., Aguzzi, A., and Weissmann, C. (2000) Prion protein devoid of the octapeptide repeat region restores susceptibility to scrapie in PrP knockout mice. *Neuron* **27**, 399–408
20. Govaerts, C., Wille, H., Prusiner, S. B., and Cohen, F. E. (2004) Evidence for assembly of prions with left-handed β -helices into trimers. *Proc. Natl. Acad. Sci. U.S.A.* **101**, 8342–8347
21. Wille, H., Bian, W., McDonald, M., Kendall, A., Colby, D. W., Bloch, L., Ollesch, J., Borovinsky, A. L., Cohen, F. E., Prusiner, S. B., and Stubbs, G. (2009) Natural and synthetic prion structure from x-ray fiber diffraction. *Proc. Natl. Acad. Sci. U.S.A.* **106**, 16990–16995
22. Cobb, N. J., Sönnichsen, F. D., McHaourab, H., and Surewicz, W. K. (2007) Molecular architecture of human prion protein amyloid. A parallel, in-register β -structure. *Proc. Natl. Acad. Sci. U.S.A.* **104**, 18946–18951
23. Lu, X., Wintrod, P. L., and Surewicz, W. K. (2007) β -Sheet core of human prion protein amyloid fibrils as determined by hydrogen/deuterium exchange. *Proc. Natl. Acad. Sci. U.S.A.* **104**, 1510–1515
24. Tycko, R., Savtchenko, R., Ostapchenko, V. G., Makarava, N., and Baskakov, I. V. (2010) The α -helical C-terminal domain of full-length recombinant PrP converts to an in-register parallel β -sheet structure in PrP fibrils. Evidence from solid state nuclear magnetic resonance. *Biochemistry* **49**, 9488–9497
25. Adrover, M., Pauwels, K., Prigent, S., de Chiara, C., Xu, Z., Chapuis, C., Pastore, A., and Rezaei, H. (2010) Prion fibrillization is mediated by a native structural element that comprises helices H2 and H3. *J. Biol. Chem.* **285**, 21004–21012
26. Kunes, K. C., Clark, S. C., Cox, D. L., and Singh, R. R. (2008) Left-handed β -helix models for mammalian prion fibrils. *Prion* **2**, 81–90
27. Lloyd, S., Mead, S., and Collinge, J. (2011) Genetics of prion disease. *Top. Curr. Chem.* **305**, 1–22
28. Priola, S. A., and Chesebro, B. (1995) A single hamster PrP amino acid blocks conversion to protease-resistant PrP in scrapie-infected mouse neuroblastoma cells. *J. Virol.* **69**, 7754–7758
29. Kaneko, K., Zulianello, L., Scott, M., Cooper, C. M., Wallace, A. C., James, T. L., Cohen, F. E., and Prusiner, S. B. (1997) Evidence for protein X binding to a discontinuous epitope on the cellular prion protein during scrapie prion propagation. *Proc. Natl. Acad. Sci. U.S.A.* **94**, 10069–10074
30. Atarashi, R., Sim, V. L., Nishida, N., Caughey, B., and Katamine, S. (2006) Prion strain-dependent differences in conversion of mutant prion proteins in cell culture. *J. Virol.* **80**, 7854–7862
31. Salamat, M. K., Dron, M., Chapuis, J., Langevin, C., and Laude, H. (2011) Prion propagation in cells expressing PrP glycosylation mutants. *J. Virol.* **85**, 3077–3085
32. Shmerling, D., Hegyi, I., Fischer, M., Blättler, T., Brandner, S., Götz, J., Rüllicke, T., Flechsig, E., Cozzio, A., von Mering, C., Hangartner, C., Aguzzi, A., and Weissmann, C. (1998) Expression of amino-terminal truncated PrP in the mouse leading to ataxia and specific cerebellar lesions. *Cell* **93**, 203–214
33. Drisaldi, B., Coomaraswamy, J., Mastrangelo, P., Strome, B., Yang, J., Watts, J. C., Chishti, M. A., Marvi, M., Windl, O., Ahrens, R., Major, F., Sy, M. S., Kretzschmar, H., Fraser, P. E., Mount, H. T., and Westaway, D. (2004) Genetic mapping of activity determinants within cellular prion proteins. N-terminal modules in PrP^C offset pro-apoptotic activity of the Doppel helix B/B' region. *J. Biol. Chem.* **279**, 55443–55454
34. Baumann, F., Tolnay, M., Brabeck, C., Pahnke, J., Klotz, U., Niemann, H. H., Heikenwalder, M., Rüllicke, T., Bürkle, A., and Aguzzi, A. (2007) Lethal recessive myelin toxicity of prion protein lacking its central domain. *EMBO J.* **26**, 538–547
35. Li, A., Christensen, H. M., Stewart, L. R., Roth, K. A., Chiesa, R., and Harris, D. A. (2007) Neonatal lethality in transgenic mice expressing prion protein with a deletion of residues 105–125. *EMBO J.* **26**, 548–558
36. Taguchi, Y., Shi, Z. D., Ruddy, B., Dorward, D. W., Greene, L., and Baron, G. S. (2009) Specific biarsenical labeling of cell surface proteins allows fluorescent- and biotin-tagging of amyloid precursor protein and prion proteins. *Mol. Biol. Cell* **20**, 233–244
37. Rutishauser, D., Mertz, K. D., Moos, R., Brunner, E., Rüllicke, T., Calella, A. M., and Aguzzi, A. (2009) The comprehensive native interactome of a fully functional tagged prion protein. *PLoS One* **4**, e4446
38. Goold, R., Rabbani, S., Sutton, L., Andre, R., Arora, P., Moonga, J., Clarke, A. R., Schiavo, G., Jat, P., Collinge, J., and Tabrizi, S. J. (2011) Rapid cell-surface prion protein conversion revealed using a novel cell system. *Nat. Commun.* **2**, 281
39. Vilette, D., Andreoletti, O., Archer, F., Madelaine, M. F., Vilotte, J. L., Lehmann, S., and Laude, H. (2001) *Ex vivo* propagation of infectious sheep scrapie agent in heterologous epithelial cells expressing ovine prion protein. *Proc. Natl. Acad. Sci. U.S.A.* **98**, 4055–4059
40. Féraudet, C., Morel, N., Simon, S., Volland, H., Frobort, Y., Créminon, C., Vilette, D., Lehmann, S., and Grassi, J. (2005) Screening of 145 anti-PrP monoclonal antibodies for their capacity to inhibit PrP^{Sc} replication in infected cells. *J. Biol. Chem.* **280**, 11247–11258
41. Moudjou, M., Treguer, E., Rezaei, H., Sabuncu, E., Neuendorf, E., Groschup, M. H., Grosclaude, J., and Laude, H. (2004) Glycan-controlled epitopes of prion protein include a major determinant of susceptibility to sheep scrapie. *J. Virol.* **78**, 9270–9276
42. Paquet, S., Langevin, C., Chapuis, J., Jackson, G. S., Laude, H., and Vilette, D. (2007) Efficient dissemination of prions through preferential transmission to nearby cells. *J. Gen. Virol.* **88**, 706–713
43. Krasemann, S., Groschup, M. H., Harmeyer, S., Hunsmann, G., and Bodeimer, W. (1996) Generation of monoclonal antibodies against human prion proteins in PrP0/0 mice. *Mol. Med.* **2**, 725–734
44. Vilotte, J. L., Soulier, S., Essalmani, R., Stinnakre, M. G., Vaiman, D., Lepourry, L., Da Silva, J. C., Bernad, N., Dawson, M., Buschmann, A., Groschup, M., Petit, S., Madelaine, M. F., Rakatobe, S., Le Dur, A., Vilette, D., and Laude, H. (2001) Markedly increased susceptibility to natural sheep scrapie of transgenic mice expressing ovine PrP. *J. Virol.* **75**, 5977–5984
45. Langevin, C., Andréoletti, O., Le Dur, A., Laude, H., and Béringue, V. (2011) Marked influence of the route of infection on prion strain apparent phenotype in a scrapie transgenic mouse model. *Neurobiol. Dis.* **41**, 219–225
46. Moudjou, M., Bernard, J., Sabuncu, E., Langevin, C., and Laude, H. (2007) Glycan chains modulate prion protein binding to immobilized metal ions. *Neurochem Int* **50**, 689–695
47. Dron, M., Dandoy-Dron, F., Farooq Salamat, M. K., and Laude, H. (2009) Proteasome inhibitors promote the sequestration of PrP^{Sc} into aggregates within the cytosol of prion-infected CAD neuronal cells. *J. Gen. Virol.* **90**, 2050–2060
48. Peretz, D., Scott, M. R., Groth, D., Williamson, R. A., Burton, D. R., Cohen, F. E., and Prusiner, S. B. (2001) Strain-specified relative conformational stability of the scrapie prion protein. *Protein Sci.* **10**, 854–863
49. Chakroun, N., Prigent, S., Dreiss, C. A., Noinville, S., Chapuis, C., Fraternali, F., and Rezaei, H. (2010) The oligomerization properties of prion protein are restricted to the H2H3 domain. *FASEB J.* **24**, 3222–3231
50. Prigent, S., and Rezaei, H. (2011) PrP assemblies. Spotting the responsible regions in prion propagation. *Prion* **5**, 69–75
51. Ben-Dor, S., Esterman, N., Rubín, E., and Sharon, N. (2004) Biases and complex patterns in the residues flanking protein N-glycosylation sites. *Glycobiology* **14**, 95–101
52. Dlouhy, S. R., Hsiao, K., Farlow, M. R., Foroud, T., Conneally, P. M., Johnson, P., Prusiner, S. B., Hodes, M. E., and Ghetti, B. (1992) Linkage of the Indiana kindred of Gerstmann-Sträussler-Scheinker disease to the prion protein gene. *Nat. Genet.* **1**, 64–67
53. Zaidi, S. I., Richardson, S. L., Capellari, S., Song, L., Smith, M. A., Ghetti, B., Sy, M. S., Gambetti, P., and Petersen, R. B. (2005) Characterization of the F198S prion protein mutation. Enhanced glycosylation and defective refolding. *J. Alzheimers Dis.* **7**, 159–171; discussion 173–180
54. Meli, M., Gasset, M., and Colombo, G. (2011) Dynamic diagnosis of familial prion diseases supports the β 2- α 2 loop as a universal interference target. *PLoS One* **6**, e19093
55. Li, J., Browning, S., Mahal, S. P., Oelschlegel, A. M., and Weissmann, C. (2010) Darwinian evolution of prions in cell culture. *Science* **327**, 869–872
56. van der Kamp, M. W., and Daggett, V. (2010) Pathogenic mutations in the

Prions with Insertions in the H2-H3 Domain

- hydrophobic core of the human prion protein can promote structural instability and misfolding. *J. Mol. Biol.* **404**, 732–748
57. Geissen, M., Mella, H., Saalmüller, A., Eiden, M., Proft, J., Pfaff, E., Schätzl, H. M., and Groschup, M. H. (2009) Inhibition of prion amplification by expression of dominant inhibitory mutants. A systematic insertion mutagenesis study. *Infect Disord. Drug Targets* **9**, 40–47
58. DeMarco, M. L., and Daggett, V. (2004) From conversion to aggregation. Protofibril formation of the prion protein. *Proc. Natl. Acad. Sci. U.S.A.* **101**, 2293–2298
59. Hafner-Bratkovic, I., Bester, R., Pristovsek, P., Gaedtke, L., Veranic, P., Gaspersic, J., Mancek-Keber, M., Avbelj, M., Polymenidou, M., Julius, C., Aguzzi, A., Vorberg, I., and Jerala, R. (2011) Globular domain of the prion protein needs to be unlocked by domain swapping to support prion protein conversion. *J. Biol. Chem.* **286**, 12149–12156